nature COMMUNICATIONS

ARTICLE

Received 22 Jan 2013 | Accepted 10 May 2013 | Published 11 Jun 2013

DOI: 10.1038/ncomms2990

OPEN

Non-volatile memory based on the ferroelectric photovoltaic effect

Rui Guo[1], Lu You[1], Yang Zhou[1], Zhi Shiuh Lim[1], Xi Zou[1], Lang Chen[1], R. Ramesh[2] & Junling Wang[1]

The quest for a solid state universal memory with high-storage density, high read/write speed, random access and non-volatility has triggered intense research into new materials and novel device architectures. Though the non-volatile memory market is dominated by flash memory now, it has very low operation speed with ~10 μs programming and ~10 ms erasing time. Furthermore, it can only withstand ~10^5 rewriting cycles, which prevents it from becoming the universal memory. Here we demonstrate that the significant photovoltaic effect of a ferroelectric material, such as $BiFeO_3$ with a band gap in the visible range, can be used to sense the polarization direction non-destructively in a ferroelectric memory. A prototype 16-cell memory based on the cross-bar architecture has been prepared and tested, demonstrating the feasibility of this technique.

[1] School of Materials Science and Engineering, Nanyang Technological University, Singapore 639798, Singapore. [2] Department of Materials Science and Engineering, and Department of Physics, University of California, Berkeley, California 94720, USA. Correspondence and requests for materials should be addressed to J.W. (email: jlwang@ntu.edu.sg).

© 2013 Macmillan Publishers Limited. All rights reserved.

There are several contenders being actively explored by the industry for the universal memory. These include resistive switching random access memory based on filamentary conduction and/or interface barrier modulation by defects[1,2], phase change memory[3,4] and magnetic random access memory, which uses tunnelling magnetoresistance effect[5,6]. Though they operate at higher speed than flash memory[7], all of them have high-energy consumption, which is detrimental for portable applications, besides other drawbacks.

A ferroelectric random access memory (FeRAM) stores information using the spontaneous polarization of ferroelectric materials. An external voltage pulse can switch the polarization between two stable directions, representing '0' and '1'. It is non-volatile and the read/write process can be completed within nanoseconds. However, despite its great promise, FeRAM has a negligible share of today's memory market, mainly due to process integration and cost issues. One problem associated with conventional FeRAM is that reading is performed by applying a bias to the ferroelectric capacitor and detecting the polarization-switching current. This process is destructive and a rewrite step is needed. Furthermore, it also requires a minimum capacitor size to generate enough current for the sensing circuit. To realize the full potential of FeRAM, it is highly desirable to have a non-destructive read-out method. Recently, the resistance change of a ferroelectric tunnel junction upon polarization reversal has been demonstrated and it can be used to sense the polarization direction non-destructively[8–10]. However, this approach requires the ferroelectric layer to be several nanometres thick at most, which poses a tremendous challenge on the device fabrication.

The photovoltaic effect has been observed in ferroelectrics several decades ago[11]. Indeed, early work had even proposed the use of the photovoltaic effect for information transfer and storage applications[12,13]. Although the maximum open circuit voltage (V_{oc}) is typically limited by the band gap of the material, in some cases, anomalously large values of V_{oc} have been reported. Recently, it was proposed that energy band bending at domain walls may be the origin of above band gap V_{oc} (ref. 14). In a ferroelectric single crystal or epitaxial film, a combination of residual depolarization field and interface depletion layers can explain the polarization-dependent photovoltaic effect[15]. $BiFeO_3$, a multiferroic material with robust ferroelectric and magnetic order at room temperature[16], and a band gap ($\sim$2.7 eV) that is within visible light range[17], offers a unique opportunity for memory application. As both signs of V_{oc} and short circuit photocurrent (I_{sc}) depend on the polarization direction[18–20], they can serve as the read-out signal in a memory device.

We have investigated the photovoltaic effect of single-domain $BiFeO_3$ films. Both V_{oc} and I_{sc} can be reversed by voltage pulses as short as 10 ns, indicating high writing speed of the memory. The data retention, fatigue performance and energy consumption of the device compare favourably with other technologies under development. A prototype memory using the cross-bar architecture has been prepared and tested. The results clearly demonstrate the feasibility of this concept.

Results

Device preparation and characterizations. Epitaxial $BiFeO_3$ films of 100 nm are grown using pulsed laser deposition (PLD) on (001) $SrTiO_3$ single-crystal substrates. We use $La_{0.7}Sr_{0.3}MnO_3$ as the bottom electrode (see Methods for details). Basic properties of the films are summarized in Supplementary Figure S1. To eliminate complications from multiple domains in $BiFeO_3$, we have used miscut substrates (4° towards (110)) to obtain single-domain films as illustrated in Fig. 1a–d. The $BiFeO_3/La_{0.7}Sr_{0.3}MnO_3$ interface at the step edge lifts the degeneracy of the multiple domains in $BiFeO_3$, and the preferred polarization direction is indicated. Following the $BiFeO_3$ deposition, an array of 5-μm × 5-μm Fe electrodes (5 nm thick) are patterned on top for subsequent electrical and photovoltaic characterizations (Supplementary Fig. S2a). Five nanometer Pt is deposited on top of Fe to prevent oxidation. Fe is chosen as the top electrode based

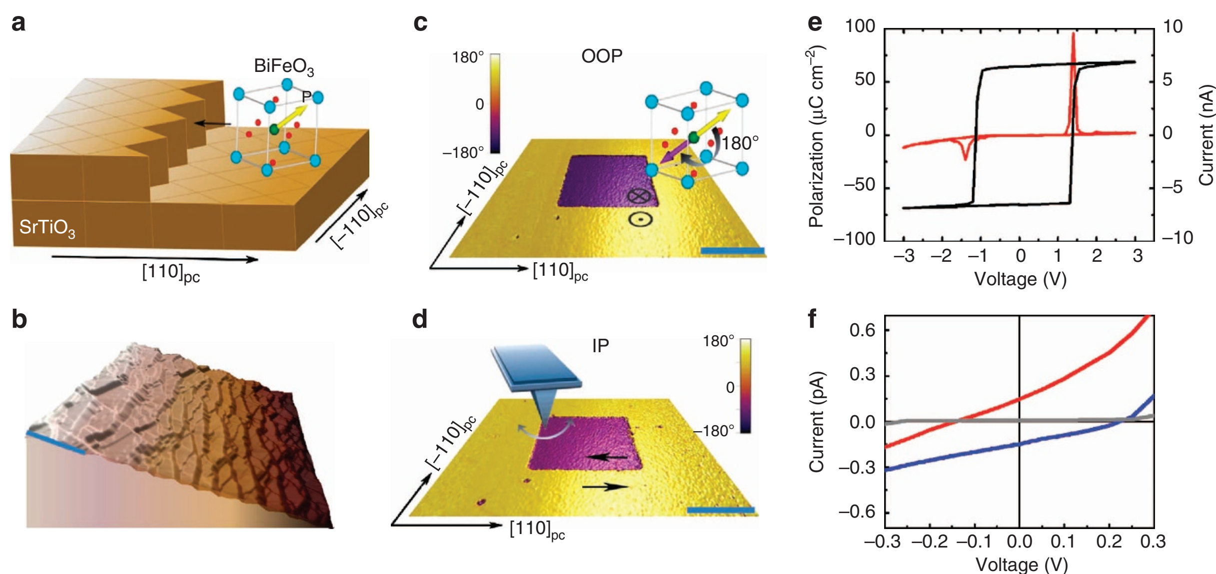

Figure 1 | Properties of as-grown $BiFeO_3$ thin films. (**a**) Schematic drawing of $BiFeO_3$ unit cell on $SrTiO_3$ substrate with 4° miscut towards (110) direction. The interface between the bottom electrode and $BiFeO_3$ at the step edge favors one of the eight degenerate polarization directions. (**b**) Topography of the $BiFeO_3$ film with steps that are clearly visible and obtained by atomic force microscopy (AFM). (**c**) Out-of-plane (OOP) and (**d**) in-plane (IP) domain images of the $BiFeO_3$ film. A 2-μm × 2-μm square region with opposite polarization direction was created by scanning the area with a DC bias applied to the AFM tip. (**e**) Typical *P–V* hysteresis loop (black) obtained at room temperature using 1 kHz triangle wave. The *I–V* curve (red) is also shown. (**f**) Current–voltage curves of the as-grown film obtained with and without illumination (grey line: in dark; red line: under light with polarization down; blue line: under light with polarization up. Light source: halogen lamp; energy density: 20 mW cm^{-2}). Scale bars, 1 μm.

© 2013 Macmillan Publishers Limited. All rights reserved.

on our investigation on the polarization fatigue in $BiFeO_3$. We have learned that charge injection at the electrode/$BiFeO_3$ interface leads to domain pinning. When the pinned domains grow across the film, macroscopic fatigue occurs[21]. Furthermore, our recent study has revealed that the Schottky barrier at the interface is critical for the charge injection process. By using a low work function metal to reduce the barrier height, charge injection can be greatly reduced and fatigue performance significantly improved[22]. The transmission coefficient of the Pt/Fe layer is about 35% within the visible spectrum (Supplementary Fig. S3).

The ferroelectric polarization–voltage (P–V) hysteresis loop shown in Fig. 1e (measured at 1 kHz. See Supplementary Fig. S4 for frequency-dependent P–V loops) reveals a remnant polarization of $\sim 65\,\mu C\,cm^{-1}$ along the $[001]_{pc}$ (the subscript pc refers to pseudo cubic) direction, consistent with earlier reports and indicative of the high quality of the films[16,23]. The coercive voltage is about 1.3 V, which can be further reduced by decreasing the film thickness or by chemical substitution in $BiFeO_3$. The applied voltage is termed as positive (negative) if a positive (negative) bias is applied to the top electrode. After poling the polarization up (down) by applying a voltage pulse of -3 V ($+3$ V), the I–V curves demonstrate clear photovoltaic effect under light (light source: halogen lamp; energy density: $20\,mW\,cm^{-2}$, which is 1/5 of one sun intensity). As shown in Fig. 1f, the V_{oc} is 0.21 V and I_{sc} is -0.15 pA for the polarization up state, and -0.13 V/0.15 pA for the polarization down state. It is thus possible to determine the polarization direction (stored information) by sensing the photovoltage or photocurrent, and this process is non-destructive. The switchable nature of the photovoltaic effect implies that it is related to the spontaneous polarization of $BiFeO_3$. This has been discussed in detail in the literature[18–20]. Basically, due to incomplete compensation of the polarization charges, the residual depolarization field is always in the opposite direction of the polarization. The depolarization field drives the photo-generated electrons and holes into opposite direction before they recombine. The asymmetric V_{oc} and I_{sc} under positive and negative polarization directions is likely due to the different work functions of the top and bottom electrodes, which also induces an internal field that does not depend on the polarization direction.

Photovoltaic behaviour. As expected, the photovoltaic response of the device depends on the intensity of the light. When the light intensity increases, both V_{oc} and I_{sc} increase (Fig. 2a–d). Although the V_{oc} saturates at $\sim$0.21 and –0.13 V, no saturation is observed for I_{sc} up to $20\,mV\,cm^{-2}$. Increasing light intensity can generate more electron-hole pairs which are separated by the internal field and lead to larger V_{oc} and I_{sc}. To assess the operation speed of the memory cells, we measure the influence of the poling pulse width on the photovoltaic response and the results are shown in Fig. 2e,f). Square pulses of 1 ns to 1 ms are used to control the polarization direction of the film, and the I–V curves under $20\,mW\,cm^{-2}$ light were measured subsequently. When 6 V pulses are applied, the spontaneous polarization starts to switch within several nanoseconds. At 10 ns, the polarization is fully reversed and both V_{oc} and I_{sc} reach expected values. This result demonstrates that the memory cell can be written within 10 ns. However, this is by no means the limit. In fact, polarization switching by pulses of <1 ns has been reported in the literature, with the ultimate limit being set by the acoustic phonon mode (velocity of sound) in the material[24]. For the reading process, as it does not require switching of polarization and the light can be kept on whenever the device is in operation, so the photovoltaic response of every cell is always ready for reading and the speed is only limited by the RC-time constant of the circuit. What's even more attractive is that, if we use V_{oc} as the sensing signal, the memory cell can be as small as lithography technique allows, as V_{oc} does not depend on the lateral size of the capacitor.

Retention and fatigue. For non-volatile memory application, long data retention and superior fatigue resistance are two critical requirements. We have monitored the V_{oc} and I_{sc} of several memory cells for 4 months, no deterioration in the signal has been observed (Fig. 3a,b). Furthermore, the memory cells have been subjected to bipolar switching for up to 10^8 cycles and show

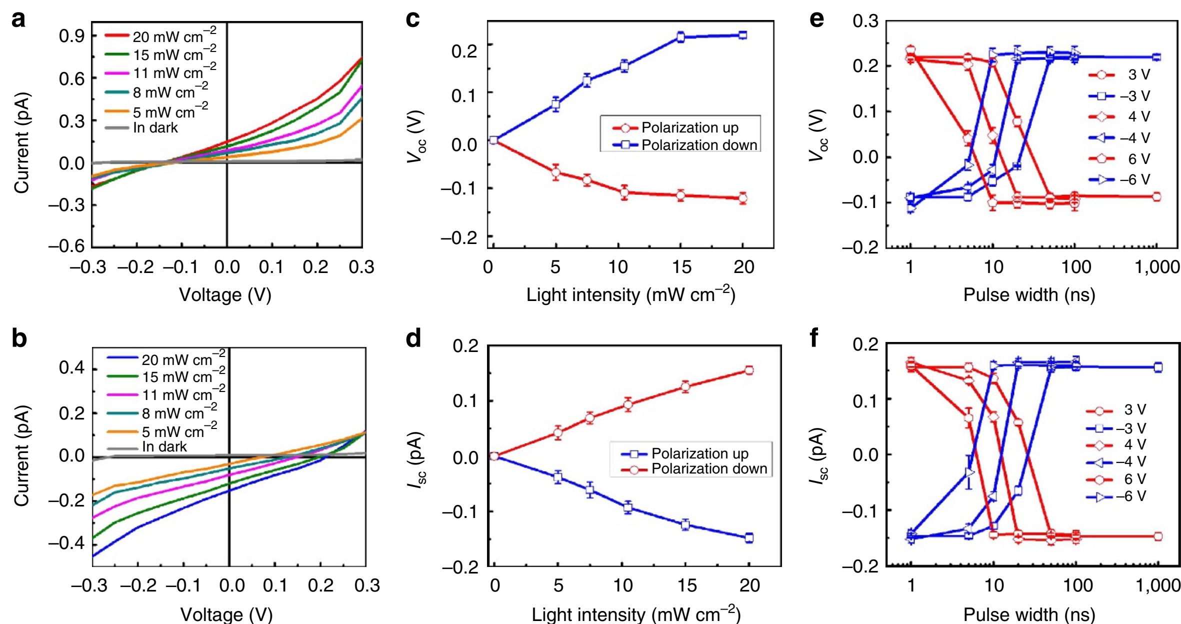

Figure 2 | Photovoltaic effect of the Fe/$BiFeO_3$/$La_{0.7}Sr_{0.3}MnO_3$/$SrTiO_3$ device. Current-voltage curves measured under different light intensity for (**a**) polarization down and (**b**) up states. (**c**) V_{oc} and (**d**) I_{sc} as functions of light intensity for both polarization directions. Pulse width dependences of (**e**) V_{oc} and (**f**) I_{sc} measured with different pulse heights.

© 2013 Macmillan Publishers Limited. All rights reserved.

no sign of fatigue (Fig. 3c–f). It is also well known in the ferroelectric community that fatigue can be mitigated by using oxide electrodes, suggesting that the non-volatile memory can sustain much more read/write cycles than flash memory.

Prototype device characterization. To assess the scalability of the photovoltaic effect-based FeRAM, we have prepared and tested a prototype memory using the cross-bar architecture. The bottom $La_{0.7}Sr_{0.3}MnO_3$ film is patterned through photolithography process and etched into stripes of 2,000 μm × 10 μm. After deposition of the $BiFeO_3$ film, top Pt/Fe electrodes of the same size are prepared (see Methods for details). The measurement setup is schematically shown in Supplementary Fig. S2b. Figure 4a depicts the topographic image of the device and each junction represents a memory cell. Despite the large size of each cell, limited by our lithography facility, all of them are fully functional. After poling the polarization direction in each cell randomly, we obtain the V_{oc} under 20 mW cm^{-2} light by measuring the I–V curve of each cell. The results are shown in Fig. 4b. The absolute values are slightly different from those obtained from the single capacitors. But the results clearly demonstrate the feasibility of this concept. Typical memory performance, that is, data retention and fatigue, has been tested for the cross-bar device. The results are similar to that of the single capacitors (Supplementary Fig. S5).

A fundamental problem for the cross-bar architecture is that sneak paths may form, which bypass the target memory cell being addressed. Practically, this can be prevented by integrating a transistor with each cell even though it reduces the memory density. In fact, the 1 transistor 1 capacitor structure is employed in conventional ferroelectric memory. However, in the proposed device, each cell generates V_{oc} and I_{sc} under light by itself. No external driving force is needed during the reading process. The sneak path problem is rather different from that in the memresistive cross-bar memory. Further study is underway to clarify this issue.

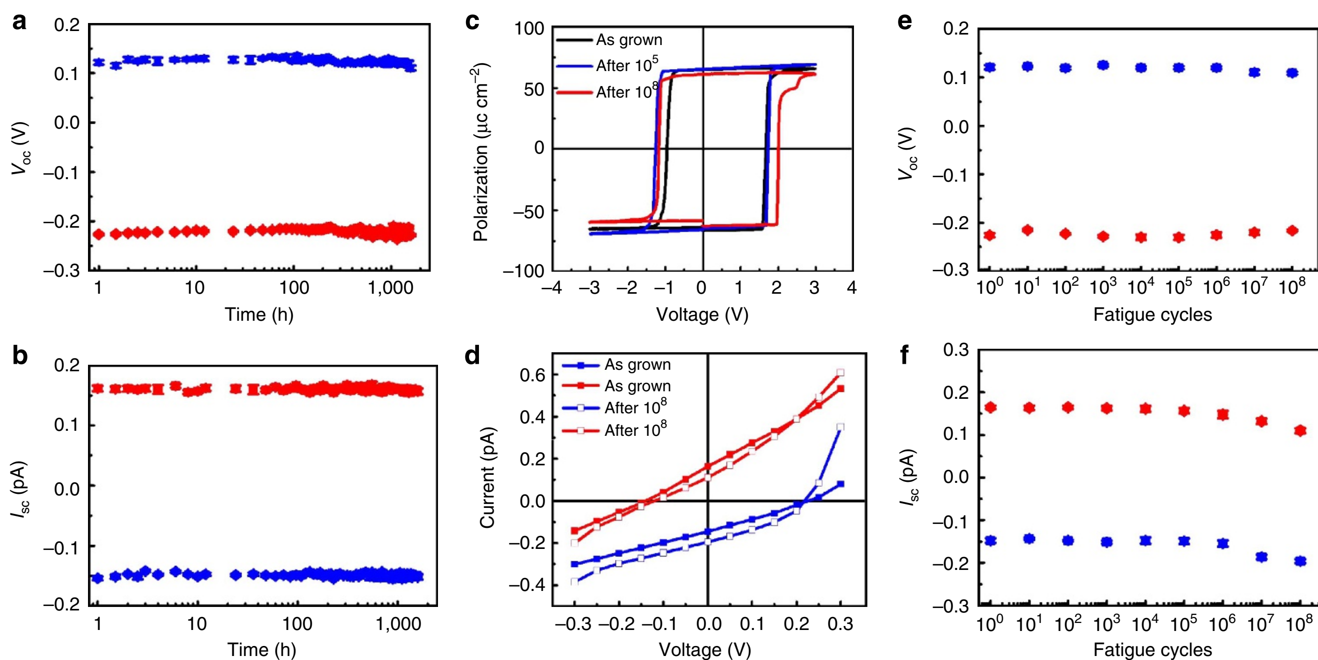

Figure 3 | Retention and fatigue behavior of the memory cell. (**a**) V_{oc} and (**b**) I_{sc} for both polarization directions show negligible change after 4 months. (**c**) P–V loops and (**d**) current-voltage curves measured after repetitive switching by pulses of ±3 V, 1 ms reveal no fatigue after 10^8 cycles. In (**a**,**b**,**d**–**f**), blue: under light with polarization up; red: under light with polarization down.

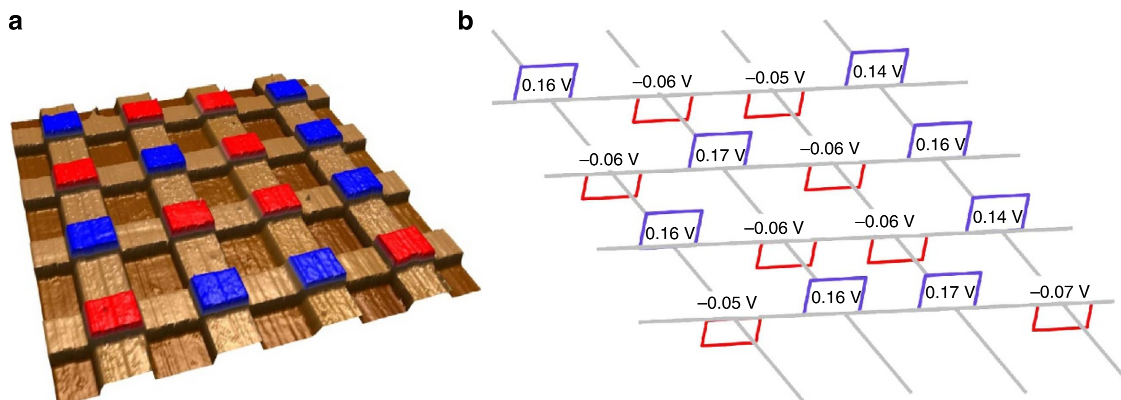

Figure 4 | Performance of a prototype 16-cell memory based on the cross-bar architecture. (**a**) Topography of the device with preset polarization direction. Blue: polarization up, red: polarization down. (**b**) V_{oc} of all 16 cells are indicated. These are measured under 20 mW cm^{-2} light.

© 2013 Macmillan Publishers Limited. All rights reserved.

Discussion

It is noteworthy that the results reported here are obtained from typical $BiFeO_3$ capacitors as proof of concept. Further optimization on the film thickness and electrode materials selection could improve the V_{oc} and the I_{sc} for better performance. For example, using electrodes with larger screening length should enhance V_{oc} due to increasing depolarization field. Furthermore, the concept is not limited to $BiFeO_3$. Other ferroelectric materials, for example, PZT and $BaTiO_3$, should give rise to similar behaviour. Compared with flash memory, the photovoltaic FeRAM reported here has much higher operation speed and lower energy consumption. It also compares favourably with other non-volatile memories that are under development currently, for example, magnetic random access memory and resistive switching random access memory (see Supplementary Table S1). In summary, we report here a novel approach to create a non-volatile memory technology that uses the polarization-dependent photovoltaic effect in ferroelectrics.

Methods

Device preparation. PLD technique was used to prepare the $La_{0.7}Sr_{0.3}MnO_3$ bottom electrode and epitaxial $BiFeO_3$ films. High-energy KrF excimer laser ($\lambda = 248$ nm) was used. $La_{0.7}Sr_{0.3}MnO_3$ of 20 nm was deposited at 670 °C with the oxygen partial pressure of 300 mTorr. The laser energy density and repetition rate were $1\,J \cdot cm^{-2}$ and 3 Hz, respectively. Following the deposition of the bottom electrode, epitaxial $BiFeO_3$ film was grown using a $Bi_{0.8}FeO_3$ target with substrate temperature of 680 °C and oxygen partial pressure of 50 mTorr. The laser energy density and repetition rate were $1\,J \cdot cm^{-2}$ and 10 Hz, respectively. After the deposition of $BiFeO_3$, photolithography was conducted to prepare the 5-μm × 5-μm top electrodes. The sample surface was first coated with a buffer layer of LOR 5 A (Microchem) using spin coater at 4,000 r.p.m., followed by baking at 110 °C for 2 min. After this, a layer of positive photoresist EPG 510 (Everlight) was coated at 4,000 r.p.m. and baked at 110 °C for 2 min. The sample was then attached to a photomask for UV light (350 W) exposure for 6 s using LithoPack 300 (SUSS MicroTec). The desired patterns were obtained by developing in TMAH (Kanto) solution for 18 s to remove the exposed photoresist. After the photolithography, Pt (5 nm)/Fe (5 nm) electrodes were deposited by PLD. The remaining photoresist was removed by a remover solution (MicroChem).

For the cross-bar device, photoresist in the shape of 2,000 μm × 10 μm stripes were created on the bottom $La_{0.7}Sr_{0.3}MnO_3$ film through photolithography. The rest of the $La_{0.7}Sr_{0.3}MnO_3$ film was etched away in a KI/HCl (1:9) solution. The remaining photoresist was removed by remover. After this, the $SrTiO_3$ substrate with $La_{0.7}Sr_{0.3}MnO_3$ electrodes was cleaned by acetone and ethanol, followed by $BiFeO_3$ deposition. The top Pt/Fe electrodes are of the same size as the bottom $La_{0.7}Sr_{0.3}MnO_3$ electrodes but in the perpendicular direction. So a capacitor of 10 μm × 10 μm is formed at each junction.

Electrical characterizations. Piezoresponse force microscopy measurement was carried out on a commercial atomic force microscope (Asylum Research MFP-3D) using Pt/Ir-coated tip. I–V curves were measured using a pA metre/direct current (DC) voltage source (Hewlett Package 4140B) on a low noise probe station. The light source was a Halogen lamp and the illumination energy density used in this study ranged from 5 to $20\,mW\,cm^{-2}$. Ferroelectric properties and switching experiments were carried out using a commercial ferroelectric tester (Radiant Technologies, Inc.) and a pulse generator (Keithley 3401).

References

1. Yang, J. J. *et al.* Memristive switching mechanism for metal/oxide/metal nanodevices. *Nat. Nanotech.* **3,** 429–433 (2008).
2. Waser, R. & Aono, M. Nanoionics-based resistive switching memories. *Nat. Mater.* **6,** 833–840 (2007).
3. Wuttig, M. & Yamada, N. Phase-change materials for rewriteable data storage. *Nat. Mater.* **6,** 824–832 (2007).
4. Kolobov, A. V. *et al.* Understanding the phase-change mechanism of rewritable optical media. *Nat. Mater.* **3,** 703–708 (2004).
5. Chappert, C., Fert, A. & Van Dau, F. N. The emergence of spin electronics in data storage. *Nat. Mater.* **6,** 813–823 (2007).
6. Åkerman, J. Toward a universal memory. *Science* **308,** 508–510 (2005).
7. Shim, S. I., Yeh, F. C., Wang, X. W. & Ma, T. P. SONOS-type flash memory cell with metal/Al_2O_3/SiN/Si_3N_4/Si structure for low-voltage high-speed program/erase operation. *IEEE Elec. Dev. Lett.* **29,** 512–514 (2008).
8. Chanthbouala, A. *et al.* Solid-state memories based on ferroelectric tunnel junctions. *Nat. Nanotech.* **7,** 101–104 (2011).
9. Garcia, V. *et al.* Giant tunnel electroresistance for non-destructive readout of ferroelectric states. *Nature* **460,** 81–84 (2009).
10. Gajek, M. *et al.* Tunnel junctions with multiferroic barriers. *Nat. Mater.* **6,** 296–302 (2007).
11. Brody, P. & Crowne, F. Mechanism for the high voltage photovoltaic effect in ceramic ferroelectrics. *J. Electron. Mater.* **4,** 955–971 (1975).
12. Brody, P. Ferroelectric photovoltaic method and apparatus for transferring information. US Patent US4103341 (1978).
13. Thakoor, A. P. & Thakoor, S. Thin film ferroelectric electro-optic memory. US Patent US005206829A (1993).
14. Yang, S. Y. *et al.* Above-bandgap voltages from ferroelectric photovoltaic devices. *Nat. Nanotech.* **5,** 143–147 (2010).
15. Yuan, G. L. & Wang, J. L. Evidences for the depletion region induced by the polarization of ferroelectric semiconductors. *Appl. Phys. Lett.* **95,** 252904 (2009).
16. Wang, J. *et al.* Epitaxial $BiFeO_3$ multiferroic thin film heterostructures. *Science* **299,** 1719–1722 (2003).
17. Ihlefeld, J. F. *et al.* Optical band gap of $BiFeO_3$ grown by molecular-beam epitaxy. *Appl. Phys. Lett.* **92,** 142908–142903 (2008).
18. Choi, T., Lee, S., Choi, Y. J., Kiryukhin, V. & Cheong, S. W. Switchable ferroelectric diode and photovoltaic effect in $BiFeO_3$. *Science* **324,** 63–66 (2009).
19. Ji, W., Yao, K. & Liang, Y. C. Bulk photovoltaic effect at visible wavelength in epitaxial ferroelectric $BiFeO_3$ thin films. *Adv. Mater.* **22,** 1763–1766 (2010).
20. Yi, H. T., Choi, T., Choi, S. G., Oh, Y. S. & Cheong, S. W. Mechanism of the switchable photovoltaic effect in ferroelectric $BiFeO_3$. *Adv. Mater.* **23,** 3403–3407 (2011).
21. Zou, X. *et al.* Mechanism of Polarization Fatigue in $BiFeO_3$. *ACS Nano* **6,** 8997–9004 (2012).
22. Zhou, Y. *et al.* Mechanism of polarization fatigue in BiFeO3: the role of Schottky barrier. Preprint at http://arxiv.org/abs/1304.7935 (2013).
23. Baek, S. H. *et al.* Ferroelastic switching for nanoscale non-volatile magnetoelectric devices. *Nat. Mater.* **9,** 309–314 (2010).
24. Li, J. *et al.* Ultrafast polarization switching in thin-film ferroelectrics. *Appl. Phys. Lett.* **84,** 1174–1176 (2004).

Acknowledgements

This work is supported by National Research Foundation of Singapore under project NRF-CRP5-2009-04. R.R. acknowledges partial support from the NSF E3S Center.

Author contributions

J.W. conceived and designed the experiments. R.G. prepared the films and devices. R.G., L.Y., Y.Z., Z.S.L. and X.Z. conducted the electrical and photovoltaic characterizations. R.G., L.C., R.R. and J.W. wrote the paper. All the authors discussed the results and commented on the manuscript.

Additional information

Supplementary Information accompanies this paper at http://www.nature.com/naturecommunications

Competing financial interests: The authors declare no competing financial interests.

Reprints and permission information is available online at http://npg.nature.com/reprintsandpermissions/

How to cite this article: Guo, R. *et al.* Non-volatile memory based on the ferroelectric photovoltaic effect. *Nat. Commun.* 4:1990 doi: 10.1038/ncomms2990 (2013).

This work is licensed under a Creative Commons Attribution-NonCommercial-ShareAlike 3.0 Unported License. To view a copy of this license, visit http://creativecommons.org/licenses/by-nc-sa/3.0/

© 2013 Macmillan Publishers Limited. All rights reserved.